Available online at www.sciencedirect.com
SCIENCE DIRECT®
Journal of Organometallic Chemistry 691 (2006) 994–1006
Journal of Organometallic Chemistry
www.elsevier.com/locate/jorganchem

Organometallic modification approach to the control of push–pull architectures: Synthesis, properties and radical polymerization of chromium *N*-vinylcarbazole derivatives

Xiaohui Tian *, Wei Shi, Kanyi Shen, Chenyan Li, Jiaping Lin, Yanchao Che, Ping Zhang

School of Materials Science and Engineering, East China University of Science and Technology, 130 Meilong Road, Shanghai 200237, China

Received 30 September 2005; received in revised form 29 October 2005; accepted 29 October 2005
Available online 5 December 2005

Abstract

In an effort to combine the donor character of the carbazole unit with the electron-withdrawing nature of the chromiumtricarbonyl moiety, which can be further modified by exchange of the CO ligand, a new series of vinyl-type monomers with organometallic push–pull chromophores, (*N*-vinylcarbazole)$Cr(CO)_2L$ (L = CO (**2**), PPh_3 (**4**), $(C_3H_5)^+BF_4^-$ (**5**)) and (*N*-vinylcarbazole)bis$Cr(CO)_3$ (**3**), have been synthesized and isolated, wherein **2** could be converted into **3** under appropriate conditions. All compounds were characterized spectroscopically, and X-ray crystal structure analyses were performed for **2**–**4**. The coordination-induced geometrical changes occur predominantly on the N-center and its attached double bond. PPh_3 replaces a CO group leading to the *N*-vinyl double bond length shortening from 1.274 (12) to 1.245 (9) Å. The distance of Cr from the carbazole plane, which allows estimates of the strength of the metal–ligand π-bonding, is shorter in **3** than in **2** as a result of an electronic communication between the two $Cr(CO)_3$ groups on each aryl ring of carbazole molecule. Electronic absorption and fluorescence spectral features of these complexes have been studied in terms of the electronic nature of the ligands. The change from **2** to **3** causes a subtle red-shift of the absorption bands due to the electronic transitions within dinuclear-carbazole ring system. The polymerization studies of these complexes under free-radical conditions lead to a better understanding of how the organometallic moiety affects the vinyl polymerization. The intriguing effect of the organometallic moiety on the intrachain excimer formation in the resultant polymers have been shown to be likely.

Keywords: Chromium; *N*-vinylcarbazole; Push–pull architecture; Ligand exchange; Polymerization

1. Introduction

The driving force to pursue research on carbazole-containing polymers comes from both fundamental interests and practical expectations [1]. It is known that these polymers, especially those with carbazole as pendant unit or copolymers, are sensitive only in the UV region of spectra [2]. The applications of such polymers in electrophotography and related process need sensitization to the visible wavelengths. Most of these efforts have been focused on charge-transfer (CT) formation in conventional organic systems [3]. Far fewer systems are known that contain organometallic subunits to control polymer properties. Incorporation of metallic center into a carbazole system through a variety of novel attachment profiles seems to be another route in designing and synthe- sizing new types of carbazole-based polymers with improved materials properties unobtainable in simple π-organic structure. The two coplanar aryl rings of carbazole unit should be able to provide a platform for transition metal π-coordination since they bond tenaciously to a wide variety of transition metal complexes [4]. In regard to the electron-withdrawing nature of the $Cr(CO)_3$ moiety which is comparable to that of a nitro substituent, coordination of $Cr(CO)_3$ to carbazole ligand

* Corresponding author. Tel./fax: +86 21 5428 8175.
E-mail address: tianxh@263.net (X. Tian).

0022-328X/$ - see front matter © 2005 Elsevier B.V. All rights reserved.
doi:10.1016/j.jorganchem.2005.10.052

could yield an organometallic push–pull structure [5] and thus, the electron cloud movement or the charge-transfer electron density from the carbazole moiety to the carbonyl groups through the metal center will make the molecule exhibit high polarizabilities, facile excitation upon irradiation with visible light and stable species of higher oxidation states. As shown by the recent reports of Merlic and other researchers [6], chromium complexation leads to strong stabilization of both benzylic anions and cations, and a high quantum yield of charge separation is achieved through field and inductive effects allowing the transition metal to participate, yet maintain an 18-electron configuration. Kobayashi et al. [7] reported on the CT complexes of areneCr(CO)$_3$ with various π-acceptors (e.g., 1,3,5-trinitro-benzene and tetracyanoethylene), in which the areneCr(CO)$_3$ behaved as electron donor with the ionization potential being ~1.5 eV lower than that of the free ligand mainly due to metal d-lone pair. Considering the great structural and electronic diversity available in the metal–organic environments, a profound understanding of the unique mode of (carbazole)Cr(CO)$_3$ and other synthetically relevant systems for the development of advanced electroactive, optical, magnetic, or catalytic materials is desired. On the other hand, the chromium atom might be tuned to act as an intermediary between donor and acceptor moieties by replacing a CO group with other ligands, for example, PPh_3 and $(C_3H_5)^+BF_4^-$ ligands are efficient at either donating or accepting electrons relative to CO [8]. In the present paper, we give full details of the syntheses of the (*N*-vinylcarbazole)bisCr(CO)$_3$ (**3**) and (*N*-vinylcarbazole)- Cr(CO)$_2$L, where L = CO (**2**), PPh_3 (**4**) and $(C_3H_5)^+BF_4^-$ (**5**) (Scheme 1). The structural features of such complexes with various ligands are discussed in relation to their behavior in photophysics and radical polymerization. In view of the fact that some of these complexes are still active for vinyl-type polymerization [9], an extension of this research to the macromolecular level was also pursued.

2. Experimental

2.1. General procedures

Unless otherwise noted, all manipulations with air-sensitive materials were performed under a nitrogen atmosphere using standard Schlenk techniques and a Vacuum Atmospheres drybox. Solvents were freshly distilled over appropriate drying reagents, and all Schlenk flasks were flame-dried under vacuum prior to use. Cr(CO)$_6$ (99%, Strem Chemicals) was sublimed prior to use. Commercial azobisisobutyronitrile (AIBN) was recrystallized three times from methanol before use (m.p.: 102–103 °C (dec)). *N*-Vinylcarbazole (**1**) (99%, Aldrich) was used as received. Commercially available poly(*N*-vinylcarbazole) (PVK) was dissolved in benzene and precipitated out with methanol numerous times to free it from residual monomer and anthracene. Column chromatography was performed on Matrix silica 60 (30–70 μm). Melting points were measured using a Reichert Thermopan melting point microscope and are uncorrected. All the crystalline chromium complexes can be handled in air. NMR spectra were recorded on a Bruker AVANCE 500 spectrometer. Chemical shifts are referenced in ppm to internal Me_4Si for the ^1H and ^{13}C NMR spectra and to external 85% H_3PO_4 and 80% CF_3COOH for the ^{31}P and ^{19}F NMR spectra, respectively. IR spectra were recorded on a Nicolet

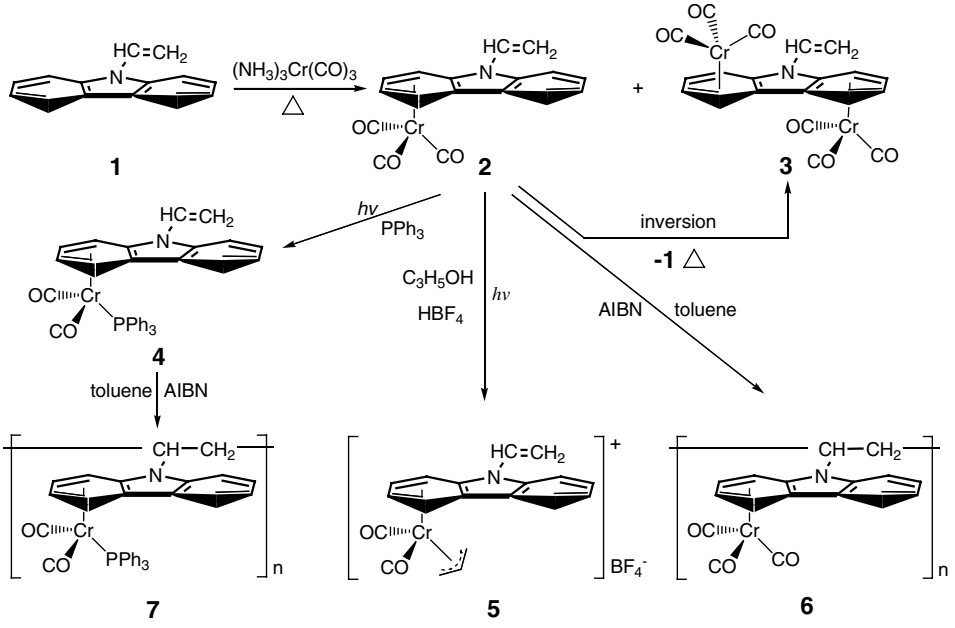

Scheme 1.

Magna-IR 550 instrument in KBr pellets. Elemental analyses were carried out on an Elementar Vario EL III analyzer (C, H and N) and TJARIS 1000 (Cr and P), respectively. Electron-impact mass spectra were recorded on a Micromass GCT (EI, 70 eV) mass spectrometer. Molecular weight measurements were carried out in a PE Series 200 gel permeation chromatograph (GPC) with polystyrene as the standard, using THF as the eluent (30 °C) at a flow rate of 1 mL/min. Thermogravimetric analyses (TGA) were carried out using a TGA SDTA 851^e instruments with a heating rate of 10 °C/min in a nitrogen flow (20 mL/min). The DSC-200 PC of TA instruments were used to measure the glass transition temperature (T_g) of the samples under nitrogen at a heating rate of 10 °C/min from −5 to 300 °C. UV–Vis spectra were obtained on a Varian Cary 500 spectrophotometer rebuilt by OLIS to incorporate computer control. Fluorescence spectra were recorded on a FLS920 spectrophotometer (EDINBURGH Instruments Ltd.) under the control of a Pentium-based PC running the SpectraCalc software package. Excitation was provided by a Xe 900 lamp operating at a current of 5 A. Fluorescence quantum yields were obtained by comparison of the integrated area of the corrected emission spectrum of the samples with that of a solutions of quinine sulfate in 1 N H_2SO_4, which has a quantum efficiency of 0.55. The concentration of the reference was adjusted to match the absorbance of the test sample. Emissions for **1**–**4** and **6** were integrated from 340 to 450 nm, and emissions for **5**, **7** and PVK were integrated from 340 to 550 nm. Measurements were made on argon saturated samples at room temperature.

2.2. Crystallography

Single crystals of **1**–**4** suitable for X–ray diffraction were obtained by recrystallization from CH_2Cl_2/*n*-hexane at −5 °C under an inert atmosphere and were sealed in thin-walled glass capillaries. Data were collected on a Bruker Smart Apex CCD diffractometer with graphite-monochromated Mo Kα radiation, $\lambda = 0.71073$ Å, using the ω–2θ technique at 293 K. All structures were solved by direct methods using SHELXS97 and refined by the full-matrix least-squares method on all F^2 data using the program SHELXL97 [10]. There are two independent molecules in the asymmetric unit of **1**. All non-hydrogen atoms were refined anisotropically. Hydrogen atoms were inserted in idealized positions and refined using a riding model. Relevant crystallographic information is summarized in Table 1.

Table 1
Details of data collection and structure refinement for **2**–**4**

	2	**3**	**4**
Empirical formula	$C_{17}H_{11}NO_3Cr$	$C_{20}H_{11}NO_6Cr_2$	$C_{34}H_{26}NO_2PCr$
Formula weight	329.27	465.30	563.53
Crystal system	Monoclinic	Triclinic	Triclinic
Space group	C2	$P\bar{1}$	$P\bar{1}$
Color, form	Orange plates	Orange needles	Violet blocks
a (Å)	13.1714(17)	7.5498(15)	7.9481(8)
b (Å)	13.8190(17)	9.826(2)	9.2605(10)
c (Å)	9.4899(12)	13.705(3)	19.818(2)
α (°)	90	69.422(2)	83.487(2)
β (°)	121.947(3)	74.322(4)	80.757(2)
γ (°)	90	86.268(4)	72.148(2)
V (Å^3)	1465.7(3)	915.9(3)	1367.2(2)
Z	4	2	2
d (calcd) (g · cm^{-3})	1.492	1.687	1.369
Absorption coefficient (mm^{-1})	0.791	1.225	0.509
F(000)	672	468	584
Crystal size (mm)	0.356 × 0.321 × 0.231	0.516 × 0.167 × 0.060	0.495 × 0.338 × 0.207
θ Range (°)	2.34–28.85	1.65–27.00	1.04–27.00
No. of reflections collected	4515	5449	8024
No. of unique data	3130	3898	5775
No. of data/restraints/parameters	3130/8/199	3098/0/262	5775/0/351
R_{int}	0.0345	0.0884	0.0642
GOF/F^2	0.928	1.170	0.965
R indices [$I > 2\sigma(I)$]	$R_1 = 0.0593$ $\omega R_2 = 0.1287$	$R_1 = 0.0636$ $\omega R_2 = 0.1646$	$R_1 = 0.0538$ $\omega R_2 = 0.1372$
R indices (all data)[a,b]	$R_1 = 0.0868$ $\omega R_2 = 0.1422$	$R_1 = 0.0731$ $\omega R_2 = 0.1746$	$R_1 = 0.0730$ $\omega R_2 = 0.1516$
Largest diff. peak and hole (e Å^{-3})	0.548/−0.235	1.310/−0.584	0.910/−0.397

[a] $R_1 = \sum ||F_o| - |F_c|| / \sum |F_o|$.
[b] $\omega R_2 = \left\{ \sum [\omega (F_o^2 - F_c^2)^2] / \sum [\omega (F_o^2)^2] \right\}^{1/2}$.

2.3. Synthesis of mono- (**2**) and bis-$Cr(CO)_3$ (**3**) complexes of N-vinylcarbazole

$Cr(CO)_6$ was reacted to give $(NH_3)_3Cr(CO)_3$ according to a literature method [5a]. A mixture of 10.3 g (55.0 mmol) of $(NH_3)_3Cr(CO)_3$ and 3.0 g (15.5 mmol) of **1** was heated under reflux in 200 mL of dioxane for 6 h. After being cooled, the solution was filtered through a celite filter and the residue was extracted into 5 mL of CH_2Cl_2 and passed through a 5 cm × 35 cm column of silica gel, eluting with a CH_2Cl_2–petroleum ether mixture (1:3). Two bands were observed: the first yellow band (mononuclear complex **2**; MS (*m*/*z*): 329 [M^+]) was collected with ~500 mL of the eluent, and the second orange band (dinuclear complex **3**; MS (*m*/*z*): 465 [M^+]) with ~300 mL of CH_2Cl_2. The products were recrystallized five times from CH_2Cl_2/*n*-hexane (3:1), respectively, to obtain two kinds of light orange crystals.

2.4. Complex **2**

Yield: 2.19 g (43.1%); m.p.: 125 °C. Anal. Calc. for $C_{17}H_{11}NO_3Cr$: C, 62.01; H, 3.37; N, 4.25; Cr, 15.79. Found: C, 62.21; H, 3.33; N, 4.11; Cr, 16.02. ^{1}H NMR ($CDCl_3$, 500 MHz): $\delta = 5.39$ (d, $J = 8.5$ Hz, 1 H), 5.45 (t, $J = 6.0$ Hz, 1 H), 5.72 (d, $J = 16.0$ Hz, 1 H), 5.92 (t. $J =$ 6.1 Hz, 1 H), 6.56 (d, $J = 6.5$ Hz, 1 H), 7.06 (d, $J =$ 6.1 Hz, 1 H), 7.31 (t, $J = 7.7$ Hz, 1 H), 7.37 (t, $J =$ 6.5 Hz, 1 H), 7.57 (t, $J = 7.5$ Hz, 1 H), 7.74 (d, $J =$ 8.0 Hz. 1 H), ^{13}C NMR ($CDCl_3$, 125 MHz): $\delta = 77.65$ (CH_2), 87.47, 89.77, 93.79, 94.50 (Ar-C), 106.12, 111.67 (Ar-C_q), 120.69 (CH), 121.21, 122.55, 123.98, 128.50 (Ar-C), 129.00, 141.49 (Ar-C_q), 234.53 (CO). EI MS (70 eV. *m*/*z* (%)): 329 (M^+, 43), 301 ($M^+ - CO$, 4), 273 ($M^+ - 2CO$, 52), 245 ($M^+ - 3CO$, 100), 193 ($M^+ - Cr(CO)_3$, 35), 52 (Cr^+, 79). IR (KBr): $\nu = 1966$, 1872, 1639, 1612, 1544, 1466, 1442, 1010, 741 cm^{-1}.

2.5. Complex **3**

Yield: 0.28 g (4.0%); m.p.: 220 °C (dec); Anal. Calc. for $C_{20}H_{11}NO_6Cr_2$: C, 51.58; H, 2.36; N, 3.01; Cr, 22.35. Found: C, 51.54; H, 2.31; N, 2.29; Cr, 22.17. ^{1}H NMR ($CDCl_3$, 500 MHz): $\delta = 5.10$ (t, $J = 6.3$ Hz, 2 H), 5.57–5.60 (m, 3 H), 5.67 (dd, $J = 14.2$ Hz, 1 H), 5.88 (d, $J = 6.8$ Hz, 2 H), 6.38 (d, $J = 6.3$ Hz, 2 H), 6.75 (dd, $J = 8.5$ Hz, 1 H). ^{13}C NMR ($CDCl_3$, 125 MHz): $\delta = 75.12$, 85.68, 86.32 (Ar-C), 91.73 (CH_2), 92.65 (Ar-C_q), 112.53 (Ar-C), 122.13 (CH), 127.08 (Ar-C_q), 232.30 (CO). EI MS (70 eV. *m*/*z* (%)): 465 (M^+, 9), 409 ($M^+ - 2CO$, 6), 381 ($M^+ - 3CO$, 7), 353 ($M^+ - 4CO$, 7), 325 ($M^+ - 5CO$, 29), 297 ($M^+ - 6CO$. 23), 273 ($M^+ - 2CO\text{-}Cr(CO)_3$, 8), 245 ($M^+ - 3CO - Cr(CO)_3$, 100), 193 ($M^+ - 2Cr(CO)_3$, 16), 52.0 ($Cr^+$, 96). IR (KBr): $\nu = 1937$, 1899, 1881, 1851, 1639, 1564, 1473, 1428, 815 cm^{-1}.

2.6. Conversion of **2** into **3** in dioxane

2 (10.0 mmol, 3.3 g) was dissolved in 800 mL of degassed dioxane, and the solution was then introduced in equal portions into eight glass tubes, which were sealed and left to stand for different time intervals at high temperature (80 °C) with avoiding sunlight. After respective time intervals, volatiles were removed in vacuo and the crude yellow solid was separated by column chromatography. Three fractions (**1**–**3**) were obtained, quantified and identified by ^{1}H NMR, respectively.

2.7. Attempted conversion of **3** into **2** in the solution

Treatment of **3** was performed analogously to that of **2**. Even after heating **3** in dioxane at 80 °C for more than 120 h, spectral evidence for the process of **3** → **2** was absent.

2.8. Synthesis of N-vinylcarbazole $Cr(CO)_2PPh_3$ complex (**4**)

2 (0.33 g, 1 mmol) and triphenylphosphine (0.79 g, 3.0 mmol, recrystallized from ethanol) were irradiated in 45 mL of dry benzene in a Schlenk tube under a Hanovia ultraviolet lamp for 8 h. The heat from the lamp was allowed to reflux the reaction mixture, and good stirring was maintained under a nitrogen atmosphere. The dark violet solution was filtered hot through a glass frit and rinsed with *n*-hexane to obtain 0.17 g (31%) of a violet solid which is stable to air. Recrystallization in dry, degassed CH_2Cl_2/*n*-hexane (3:1) yielded large, dark violet crystals; m.p.: 168 °C (dec); Anal. Calc. for $C_{34}H_{26}NO_2PCr$: C, 72.47; H, 4.62; N, 2.49; Cr, 9.24. Found: C, 72.42; H 4.45; N 2.28; Cr 9.03. ^{31}P NMR (C_6D_6, 202 MHz): $\delta = 90.82$ (s, br). ^{1}H NMR (C_6D_6, 500 MHz): $\delta = 4.25$ (s, 1 H), 4.66 (s, 1 H), 4.72 (d, $J = 8.7$ Hz. 1 H), 4.97 (d, $J = 5.1$ Hz, 1 H), 5.15 (s, 1 H), 5.19 (d, $J = 13.0$ Hz, 1 H), 6.49 (d, $J = 9.0$ Hz, 1 H), 6.95 (s, 10 H), 7.15 (s, 2 H), 7.23 (d, $J = 7.2$ Hz, 1 H), 7.38 (s, 6 H). ^{13}C NMR (C_6D_6, 125 MHz): $\delta = 71.90$, 84.72, 86.72, 88.59 (Ar-C), 90.31 (CH_2), 104.59, 111.09 (Ar-C_q), 118.72 (CH), 120.84, 121.87, 125.85 (Ar-C), 128.50 (Ar-C_q), 129.32 (Ar-C), 133.83 (Ar-C_q), 133.92, 140.40 (Ph-C). 241.70 (CO). EI MS (70 eV, m/z (%)): 563 (M^+, 5), 507 ($M^+ - 2CO$, 49), 314 ($CrPPh_3^+$, 100), 262 (PPh_3^+, 20), 193 ($M^+ - Cr(CO)_2PPh_3$, 46), 52 (Cr^+, 38), IR (KBr): $\nu = 1865$, 1822, 1647, 1546, 1465, 1430, 1295, 1096, 747 cm^{-1}.

2.9. Synthesis of N-vinylcarbazole $Cr(CO)_2(C_3H_5)^+BF_4^-$ (**5**)

2 (0.53 g, 1.6 mmol) and dry ethyl ether (80 mL) were placed into a 250-mL round-bottom flask. A solution of 50% aqueous HBF_4 (0.28 g, 1.6 mmol) and allyl alcohol (0.12 g, 2.0 mmol) in 40 mL of ethyl ether was added. The solution was irradiated with a Hanovia ultraviolet lamp

under a nitrogen atmosphere. The flask was cooled with a rapid stream of air to prevent any decomposition from occurring. After 3–4 h of irradiation, the solution was filtered under nitrogen leaving insoluble **5** as a brick red solid (ca. 0.16 g, 23% yield), which was completely redissolved in about 15 mL of dry acetone. Analytically pure samples were obtained by numerous reprecipitations from the acetone/ether mixture; m.p.: 155–157 °C decompose without melting. Anal. Calc. for $C_{19}H_{16}O_2NBF_4Cr$: C, 53.15; H, 3.73; N, 3.26; Cr, 12.12. Found: C, 53.10; H, 3.12; N, 3.13; Cr, 11.96. ^{19}F NMR ($(CD_3)_2CO$, 471 MHz): $\delta = 151.30$ (s, br). ^1H NMR ($(CD_3)_2CO$, 500 MHz): $\delta = 1.10$ (d, $J = 6.7$ Hz, 1 H), 1.22 (d, $J = 10.4$ Hz, 1 H), 3.52 (dd, $J = 14.0$ Hz, 2 H), 3.77 (s, 1 H), 5.80 (d, $J = 8.2$ Hz. 1 H), 6.04 (d, $J = 15.7$ Hz, 1 H), 6.63 (s, 1 H), 6.94 (s, 1 H), 7.55 (dd, $J = 8.9$ Hz, 1 H), 7.69 (s, 1 H), 7.76 (d, $J = 6.7$ Hz, 1 H), 7.96 (t, $J = 6.7$ Hz, 1 H), 8.08 (t, $J = 10.1$ Hz, 2 H), 8.52 (d, $J = 7.1$ Hz, 1 H). ^{13}C NMR ($(CD_3)_2CO$, 125 MHz): $\delta = 56.96$, 57.25 (CH_2), 88.72 (CH), 98.77 (CH_2), 103.50, 111.60 (Ar-C), 112.66 (CH), 113.76, 121.07 (Ar-C_q), 121.64, 124.33, 124.81, 125.17, 127.30, 128.70 (Ar-C), 132.98, 140.18 (Ar-C_q), 224.69 (CO). ESI-MS: 342.1 [$M - BF_4^-$], 771.2 [$2M - BF_4^-$]. IR (KBr): $\nu = 1997$, 1928, 1644, 1613, 1559, 1495, 1445, 1057, 751 cm^{-1}.

2.10. Polymerization reactions

The procedures for both polymerizations of **2** and **4** were essentially the same. Polymerization was carried out in freshly distilled toluene. AIBN was used as the free radical initiator. Monomers were stored at −20 °C in the dark and were freshly prepared before use.

Fischer–Porter aerosol compatible tubes with valves were used for polymerization. Weighed amounts of monomer, solvent, and initiator were charged to the tubes; the tubes were sealed and degassed at 10^{-3} mm by three alternate freeze–thaw cycles. Liquid nitrogen was used as the freezing medium. After degassing, the tubes were placed in a thermostat for a predetermined amount of time. After removal from the bath, the polymer was precipitated in rapidly swirling large excess of petroleum ether. When necessary, the polymer solution was diluted with more solvent before precipitation to obtain fine polymer particles rather than large chunks. This process was repeated three times to ensure that all monomers and other contaminants had been washed from the polymer. After precipitation the polymers were filtered and dried under vacuum. Yields were determined gravimetrically.

2.11. Poly(N-vinylcarbazole)Cr(CO)$_3$ (**6**)

Anal. Calc. for $C_{17}H_{11}NO_3Cr$: C, 62.21; H, 3.03; N, 4.20; Cr, 16.11. Found: C, 62.13; H, 3.07; N, 4.16; Cr, 15.99. ^1H NMR ($CDCl_3$, 500 MHz): $\delta = 4.26$ (s, 1 H), 4.30 (t, $J = 6.4$ Hz, 1 H), 4.72–4.78 (m, 2 H), 5.08 (dd, $J = 14.6$ Hz, 1 H), 5.18 (d, $J = 6.9$ Hz, 1 H), 5.78 (d, $J = 6.4$ Hz, 1 H), 6.33 (dd, $J = 8.9$ Hz, 1 H), 6.97–7.02 (m, 2 H), 7.45 (d, $J = 7.7$ Hz, 1 H). IR (KBr): $\nu = 1952$, 1860, 1545, 1460, 1425, 1310, 1202, 1165, 743 cm^{-1}.

2.12. Poly(N-vinylcarbazole)Cr(CO)$_2$PPh$_3$ (**7**)

Anal. Calc. for $C_{34}H_{26}NO_2PCr$: C, 72.52; H, 4.45; N, 2.28; P, 4.75; Cr, 9.43. Found: C, 72.47; H, 4.52; N, 2.09; P, 4.70; Cr, 9.24. ^1H NMR (C_6D_6, 500 MHz): $\delta = 1.40$ (s, 1 H), 2.11 (s, 1 H), 4.26 (t, $J = 5.9$ Hz, 1 H), 4.67–4.74 (m, 1 H), 5.16–5.23 (m. 1 H), 6.50 (dd, $J = 8.9$ Hz, 1 H), 6.8–7.4 (several broad peaks, 19 H), 7.82 (t, $J = 7.9$ Hz, 1 H). IR (KBr): $\nu = 1951$, 1860, 1815, 1550, 1480, 1445, 1315, 1160, 1095, 745 cm^{-1}.

3. Results and discussion

3.1. Synthesis and Structures of mono- (**2**) and bis-Cr(CO)$_3$ (**3**) complexes of N-vinylcarbazole

Treatment of *N*-vinylcarbazole (**1**) with 3 equiv of $(NH_3)_3Cr(CO)_3$ in refluxing dioxane under protection against incandescent light for 6 h lead to the precipitation of inorganic chromium and a clear deep orange solution. Filtration and partial evaporation of the solvents from the filtrate under vacuum gave a mixture of **2** and **3** with 92/8% occupancy, and they could be separated by column chromatography. An attempt to improve the yield of **3** using an excessive Cr reagent, a high boiling point solvent and longer reaction time failed. It is unclear in this reaction what factors control the yield of **3** vs. **2**, but we suspect that some of reaction mixtures (or a trace of O_2 due to non-sealed system) decelerate the formation of **3**. It is noteworthy that heating pure **2** in appropriate solvents under an inert atmosphere for several hours gives rise to a conversion to **3**. Dioxane, THF and pyridine are found to be good solvents for such conversion, probably due to their ability to induce the decomplexation of **2**, generating a labile intermediate $(solvent)_3Cr(CO)_3$, which further affords "hot" $Cr(CO)_3$ particles and randomly attacks **1** and the remaining **2** [5a,11]. Under similar conditions, we are unaware of the conversion from **3** to **2** and moreover, **3** is completely stable even at higher temperature (100 °C) for days. Kinetic curves for the conversion of **2** into **3** in dioxane at 80 °C are shown in Fig. 1. An accumulation of **1** in the system is almost comparable to equimolar amount of **3**, indicating that there is a simple equilibrium involved with little or no loss of the $Cr(CO)_3$ particles [12]. Accordingly, **2** represents the kinetically controlled product and **3** the thermodynamically controlled one. This aspect allows us to hold a new approach to synthesize the novel binuclear complexes of the type **3**.

EI-mass spectra of **1** and **2** show a peak of the highest mass corresponding to their monomeric formulas, respectively. The infrared spectra of **2** and **3** in the carbonyl stretching region are very different – two bands are seen in **2** ($\nu_{co} = 1966$, 1872 cm^{-1}), while **3** has three bands ($\nu_{co} = 1937$, 1899 and 1881 cm^{-1}), indicating some

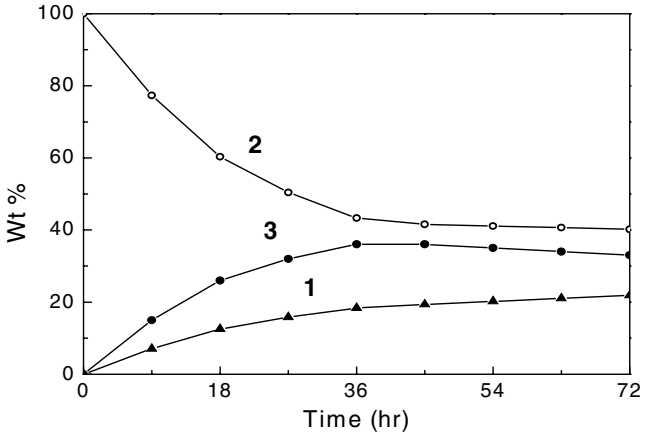

Fig. 1. Kinetic curves of conversion of **2** into **3** in dioxane at 80 °C.

coupling of the CO vibration of the two $Cr(CO)_3$ units in the latter case. NMR experiments show the general upfield shifts for all the aryl resonances in **3**, whereas **2** displays the highfield shifts only for one aryl ring. Moreover, the difference of the highfield shifts from metal coordination between **2** and **3** was noticed, further illustrating the presence of ligand-mediated metal–metal interaction for the dichromium species [13].

Complexes **2** and **3** were also characterized by X-ray crystallography, together with their organic counterpart **1** for comparative purposes. Selected bond lengths and angles are given in Table 2, and ORTEP diagrams of **1**–**3** are provided in Figs. 2–4. Crystals of **1** belong to orthorhombic system with space group $Pna2_1$, the lattice is composed of two independent molecules with distinction of the *N*-vinyl group, for example, the bond lengths of C13–C14 and C27–C28 are 1.231 (6) and 1.270 (5) Å, respectively; C14 lies 0.16 Å above the carbazole plane which is planar to within 0.03 Å, while C28 lies 0.42 Å above its carbazole plane (planar to within 0.02 Å). There are no apparent short-range intermolecular interactions between the carbazole rings. Complexes **2** and **3** crystallize in the monoclinic and triclinic system with space group $C2$ and $P\bar{1}$, respectively. Owing to the repulsive interaction between the $Cr(CO)_3$ orbitals and the central heterocycle π orbitals [4d,14], they adopt a similar exo (staggered) conformation about the Cr–$c(0)$ axis [$c(0)$ = Cr-ring centroid] such that the carbonyl ligands do not eclipse the junction C–C bond. The $Cr(CO)_3$ groups are shifted somewhat from an idealized η^6 position away from the ring junctions with the tilt angle (2.95° for **2**; 2.09° and 1.19° for **3**) between the normal to the ring plane and the line Cr–$c(0)$. Two $Cr(CO)_3$ groups in **3** are η^6-coordinated to opposite faces of an essentially planar carbazole ring, and the distances of Cr(1) and Cr(2) from the mean plane are −1.731 and 1.734 Å, which are relatively shorter than that of 1.741 Å in **2**. This may be attributed to an indirect metal–metal electronic interaction in **3** [13]. Probably the compromise

Table 2
Selected bond lengths (Å) and angles (°) for **2**–**4**

2			
N(1)–C(4)	1.436(12)	N(1)–C(15)	1.439(14)
N(1)–C(16)	1.528(13)	C(4)–C(5)	1.437(12)
C(4)–C(9)	1.408(6)	C(10)–C(15)	1.329(12)
C(16)–C(17)	1.274(12)		
C(4)–N(1)–C(15)	109.0(8)	C(5)–C(4)–C(9)	70.7(5)
C(4)–C(9)–C(8)	115.7(11)	C(11)–C(10)–C(15)	123.5(9)
C(10)–C(15)–C(14)	124.5(13)	N(1)–C(16)–C(17)	122.7(12)
3			
N(1)–C(7)	1.376(5)	N(1)–C(18)	1.392(18)
N(1)–C(19)	1.425(5)	C(7)–C(8)	1.414(5)
C(7)–C(12)	1.419(5)	C(12)–C(13)	1.450(5)
C(13)–C(18)	1.419(5)	C(17)–C(18)	1.412(5)
C(19)–C(20)	1.275(6)		
N(1)–C(7)–C(12)	110.0(3)	C(8)–C(7)–C(12)	120.2(4)
C(7)–C(12)–C(11)	120.8(3)	C(14)–C(13)–C(18)	120.3(3)
N(1)–C(18)–C(13)	109.3(3)	C(13)–C(18)–C(17)	121.0(3)
4			
Cr–P	2.2967(9)	N(1)–C(3)	1.417(4)
N(1)–C(14)	1.376(5)	P–C(17)	1.840(3)
P–C(23)	1.850(3)	P–C(29)	1.848(3)
C(15)–C(16)	1.245(9)		
Cr–P–C(17)	116.83(10)	Cr–P–C(23)	116.68(10)
Cr–P–C(29)	117.78(9)	C(18)–C(17)–C(22)	117.4(3)
C(24)–C(23)–C(28)	117.4(3)	C(30)–C(29)–C(34)	118.1(3)

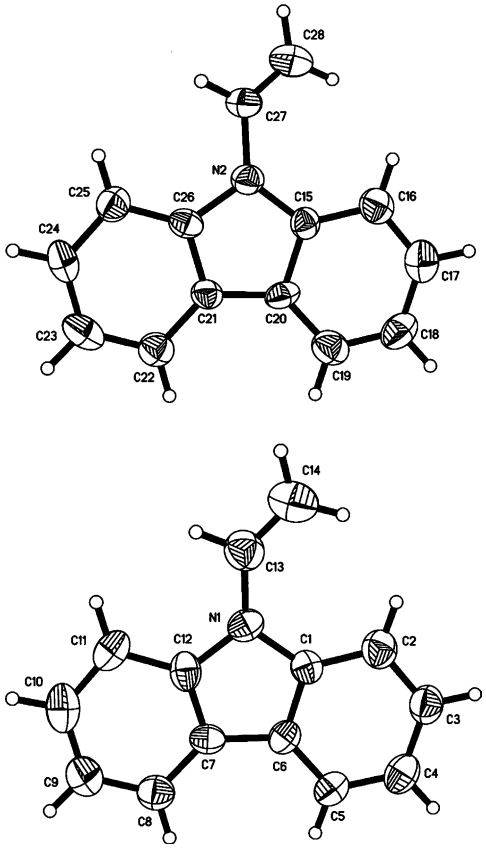

Fig. 2. ORTEP drawing of **1** with thermal ellipsoids at the 30% probability level.

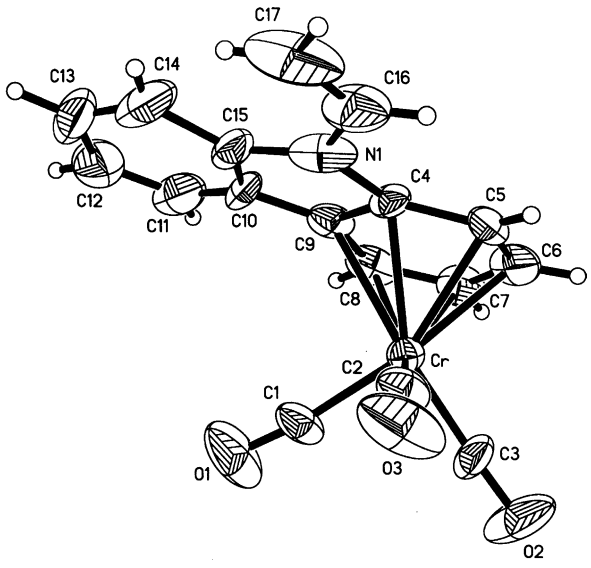

Fig. 3. ORTEP drawing of **2** with thermal ellipsoids at the 30% probability level.

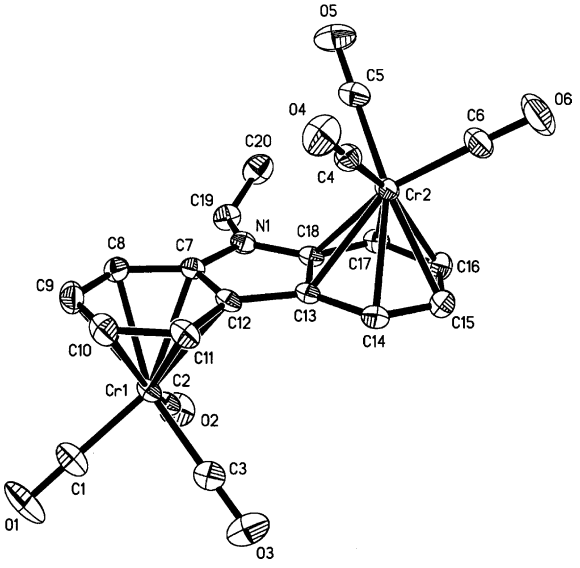

Fig. 4. ORTEP drawing of **3** with thermal ellipsoids at the 30% probability level. Hydrogen atom have been omitted for clarity.

between field and inductive effects by both metal centers is better and serves to stabilize its dinuclear-structure [6a,6b]. The carbazole fragment is found keeping the ring planar to within 0.05 Å for **2** and 0.06 Å for **3**, and the *N*-vinyl group and its attached ring in **2** are coplanar due to favorable orbital interaction. The steric crowdedness around *N* center resulting from the two $Cr(CO)_3$ groups in **3** is evidenced by the torsion angle of 146.0(5)° for C7–N–C19–C20. The N bond lengths fall into the different range (1.436(12)–1.528(13) Å for **2**; 1.376(5)–1.428(5) Å for **3**), but their attached double bond lengths (1.274 (12) Å for **2**; 1.275 (6) Å for **3**) are equal to each other and consistently longer than that observed in **1**. This is plausibly rationalized by some extent of electron transfer to the $Cr(CO)_3$ from the double bond via zwitterionic resonance form [5a,15].

3.2. Synthesis and Structures of (*N*-vinylcarbazole)Cr-$(CO)_2PPh_3$ (**4**)

Compound **2** reacted with triphenylphosphine in benzene upon simultaneous UV irradiation for 6 h to afford (*N*-vinylcarbazole)$Cr(CO)_2PPh_3$ (**4**). Analytically pure crystals were obtained in 30% yield by fractional crystallization from a mixture of dichloromethane and hexane at −30 °C. The reaction of **3** with triphenylphosphine in a similar manner has also been carried out resulting in a complex mixture which is difficult to separate. The multiple potential displacement sites are suspected to be the problems. Complex **4** is stable to air and moisture in the solid state but rapidly decomposed in solution at room temperature. The EI-mass spectrum of **4** shows a peak of the highest mass at the molecular ion [M^+] with a relative intensity of 5%. The ^{31}P NMR shows a broad singlet at 90.82 ppm. The IR spectrum gives two strong carbonyl vibronic bands at 1865 and 1822 cm^{-1} which are shifted toward lower energies (vs **2**) [8,16], suggesting that the phosphine ligand exerts its influence on the Cr center. Similar electronic effects are also noted in the ^{13}C and ^{1}H NMR chemical shifts of the Cr-ring, i.e., shifted to high field, while the carbonyl carbon resonances are slightly shifted downfield.

The structure of **4** was also determined by X-ray analysis. The crystals are triclinic, space group $P\bar{1}$. Selected bond lengths and angles are given in Table 2, and ORTEP diagrams of **4** are provided in Fig. 5. A distinguishing feature of **4** is that the rotation about the Cr–*c*(0) axis forces the Cr–P bond to the opposite position to the *N*-vinyl group in response to the steric requirements of the PPh_3 group,

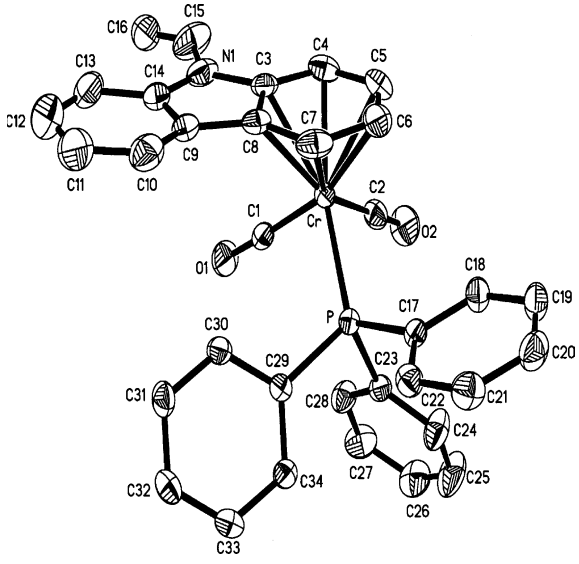

Fig. 5. ORTEP drawing of **4** with thermal ellipsoids at the 30% probability level. Hydrogen atom have been omitted for clarity.

one phenyl ring of which is less susceptible to the steric bulk and electronic influences of the Cr-ring than the other two. The Cr atom is offset slightly toward the four unsubstituted Cr-ring carbon atoms with the tilt angle of 1.94° between the normal to the ring plane and the line Cr–*c*(0). The distance of 1.736 Å from Cr to the least-squares plane is slightly longer than that found in **3** but just shorter than that found in **2**. The Cr-ring carbon bond lengths (av. 1.340 Å) are within typical ranges, which are not significantly different from that for **2**. However, the double bond length of 1.245 (9) Å in **4** is exceptionally shorter (by ca. 0.03 Å) than that in **2** and **3**. This suggests that ligand exchange on the metal moiety imposes strong influence on the double bond character, namely, the PPh_3 ligand enhances the electron density onto the *N*-vinyl group through the Cr center and thus strengthens the double bond. Further support for this viewpoint comes from an upfield shift of the $=CH_2$ group in the ^1H and ^{13}C NMR spectra (vs **2**). The out-of-plane deviation of the *N*-vinyl group is registered for its terminal carbon atom bending towards the chromium by about 0.124 Å, probably for the same reason.

3.3. Synthesis of (*N*-vinylcarbazole)$Cr(CO)_2(C_3H_5)^+BF_4^-$ (**5**)

The synthesis of (*N*-vinylcarbazole)-$Cr(CO)_2(C_3H_5)^+BF_4^-$ (**5**) was accomplished by the photochemical reaction of **2** with equimolar amounts of allyl alcohol and fluoboric acid in anhydrous ether solution for 8 h. Choice of anhydrous ether as the reaction solvent was essential because the ionic complex formed is practically insoluble in this solvent and precipitates, thus avoiding decomposition under the action of UV irradiation. After work-up, complex **5** as a brick red solid is insoluble in most of organic solvents (e.g., benzene, CH_2Cl_2, and THF) but soluble in acetone, DMSO and pyridine. The recrystallization and chromatography did not lead to further purification due to its extreme sensitivity toward air and moisture. However, its pure form could be obtained by numerous reprecipitations from the acetone/ether mixture. We tried to replace **2** by **3** in this reaction, but no bis(*N*-vinylcarbazole)$Cr(CO)_2(C_3H_5)^+BF_4^-$ complex was found as a product and the reactions involved appear to be non-specific. Complex **5** resonates at 151.3 ppm in the ^{19}F NMR spectrum. Elemental analysis is consistent with the given formulas and the ^{13}C, ^1H NMR signals for each ligand appear in their characteristic regions. Two doublets at ~1.22 ppm ($J = 6.7$–10.4 Hz) and ~3.52 ($J = 10.4$ Hz) ppm were observed for the terminal protons of the π-allyl ligand, which should be assigned to the *sin*-protons and *anti*-protons, respectively. The central proton shows itself as a broad singlet at 3.77 ppm. Compared to **2** and **4**, the resonances of the Cr-ring proton and carbon in **5** are shifted downfield and the carbonyl signals are shifted upfield due to the strong electron-withdrawing effect of the $(C_3H_5)^+BF_4^-$ ligand. Correspondingly, the ν_{CO} bands in the IR spectrum are markedly shifted toward higher frequencies at 1997 and 1928 cm^{-1}. Crystals suitable for X-ray diffraction were not obtained, despite repeated attempts. We are therefore unable to provide a reliable estimate of the metal–organic architecture for **5**. However, by analogy with the structures of **2** and **4**, it is plausible that insertion of the strongly π-accepting $(C_3H_5)^+BF_4^-$ ligand permit this species to function as extended organometallic push–pull chromophores.

3.4. Radical polymerizations

Complexes **2** and **4** were successfully polymerized in degassed toluene using recrystallized AIBN as the initiator at 80 °C to yield the corresponding well-defined poly(*N*-vinylcarbazole)$Cr(CO)_3$ (**6**) and poly(*N*-vinylcarbazole)Cr-$(CO)_2PPh_3$ (**7**). No evidence for the above-mentioned conversion of **2** into **3** has been found in toluene even after prolonged periods at elevated temperature (100 °C, 80 h). Care must be exercised at this stage to conduct the polymerization in an evacuated and sealed system to avoid decomplexation of the chromium from the carbazole ligand by photolysis under O_2. The resultant polymers **6** and **7** are moderately soluble in benzene, toluene, and chlorine-containing solvents and are film-forming materials. Additionally, these polymers are very stable toward air and moisture in the solid state and can be stored in solution in contact with air for an extended period of time without decomposition. The ^1H NMR and IR spectra of these polymers deserve comment consulting with their corresponding parent complexes. Elemental analysis data, which are included in Section 2, confirmed no loss of the metal unit from the pendant carbazole groups for each polymer. Notice in Fig. 6 that a linear M_n progression with the conversion and low polydispersity indices (PDIs) lead us to immediately suppose a stable free radical polymerization (SFRP) mechanism. To further clarify this point, we have simulated a stop-and-go experiment with these two complexes, where the polymerization was stopped by liquid

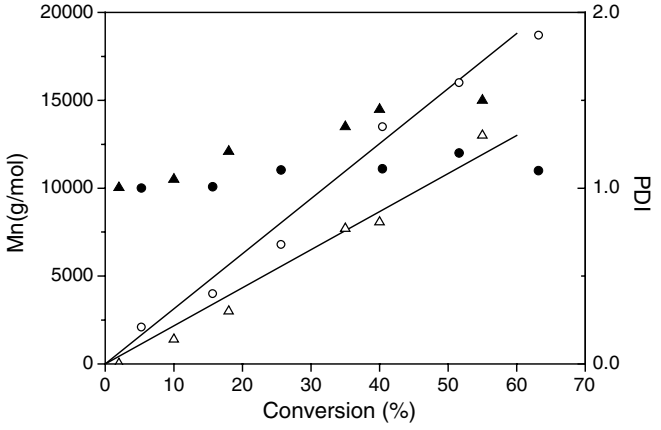

Fig. 6. Mn (left axis: open, circles for **2** and triangles for **4**) and PDI (right axis: solid, circles for **2** and triangles for **4**) as a function of conversion for The SFRP at 80 °C.

nitrogen freezing for a day and then restarted after adding a fresh aliquot of the complexes **2** and **4**, respectively (Fig. 7). The slope of the $\ln([M]_0/[M])$ vs. time plot is identical before and after the interruption within experimental error, indicating that the total number of chains is conserved. The other evidence for SFRP is the reduction of the polymerization rate and complete disappearance of the autoacceleration, which did not occur in the case of **1** (Fig. 8). This phenomenon is one of the general features of controlled radical polymerization [17]. Indeed, the polymer chain growth control is connected with the known stabilization of a free radical in the coordination sphere of the metal [18]. At the beginning of the reaction, a fast reversible equilibrium is established between a reactive free radical and a stable free radical (or persistent radical), which can be represented as a resonance structure containing an unpaired electron at the chromium atom (see Scheme 2).

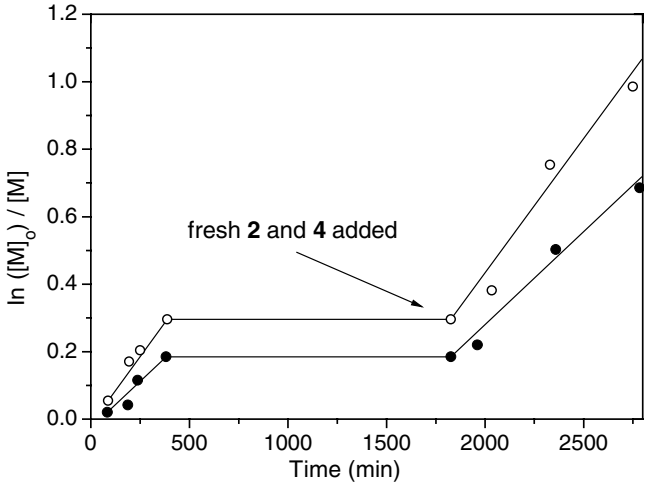

Fig. 7. Plots of $\ln([M_0]/[M])$ vs. time for the SFRP with **2** (open circles) and **4** (solid symbols).

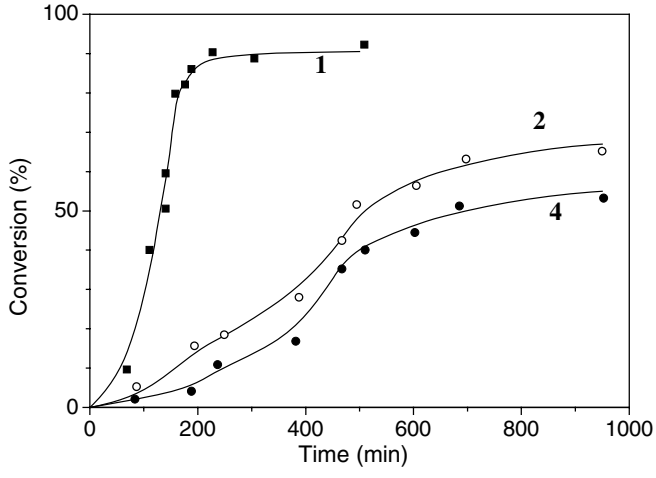

Fig. 8. Conversion vs. time for the solution polymerization at 80 °C with **1** (squares), **2** (open circles) and **4** (solid circles).

In situ the carbonyl groups and, even more strikingly, the PPh_3 group appear to form a very efficient "umbrella" over the chromium atom, making its coordination sphere practically inaccessible to attack by another reactant. For the unpaired electron transfer (through-bond) in the organometallic radical, the exocyclic N–C_α bond is essentially coplanar with carbazole ring to maximize orbital overlap and electron delocalization between the two. It is also interesting to point out that, with regard to the neighboring group participation by chromium in the *N*-vinyl reaction [8a,19], the N–C_α bond may be inclined from the carbazole plane to afford closed-shell electron configurations (through-space) at both chromium and the active carbons. As a result of the competing direct chain propagation, the M_n values of the polymers formed are consistently below 20,000. Attempts to polymerize the dinuclear complex **3** were unsuccessful even after prolonged periods at elevated temperature (100 °C, 56 h). Two $Cr(CO)_3$ groups on one carbazole ring increase steric compression and stabilization of the resulting radical to prevent the chain propagation. Complex **5** is not sufficiently stable to carry out the polymerization under those conditions. This reaction was not studied in further detail.

Polymers **6** and **7** were subjected to thermal gravimetrical analysis (TGA) under a nitrogen atmosphere. The decomposition of **7** took place in three well-separated stages with maximum rate at 240, 280 and 440 °C, in contrast to **6**, which decomposed in two stages with maximum rate at 290 and 455 °C. The IR spectrum of **7** after heating to 250 °C under nitrogen and then cooling shows no bands assignable to the CO groups, indicating that its initial weight loss was attributed to the liberation of carbon monoxide from the chromium center. Correspondingly, the second stage can be explained to result from the disruption of Cr–C (ring) bonds concomitant with the cleavage of partial P–Cr bonds [20]. Other features noted are that no clear phase transition was observed in DSC scans up to 300 °C. As with the polar, optically anisotropic chromophores as pendant groups in the side chains, these metallopolymers possess high glass transition temperature and therefore the electric field induced dipole orientation can conceivably be fixed after the film-forming, corresponding to the lowest degree of orientational relaxation. Assembled arrays of Cr-bound carbazole groups obtained in the more stable poled film make this class of materials a very competitive one for optoelectronics.

3.5. Electronic absorption and fluorescence spectroscopy

The electronic absorption spectra of the complexes have been determined to elucidate the effects of donor–acceptor properties of various ligands. The measurements were carried out using a solution of their analytically pure samples under a nitrogen atmosphere. The spectra of complexes **2** and **3** are characterized by two rather strong bands in the region of 340–355 and 395–440 nm (Fig. 9). The lower energy bands are assigned to the metal-to-ligand charge-

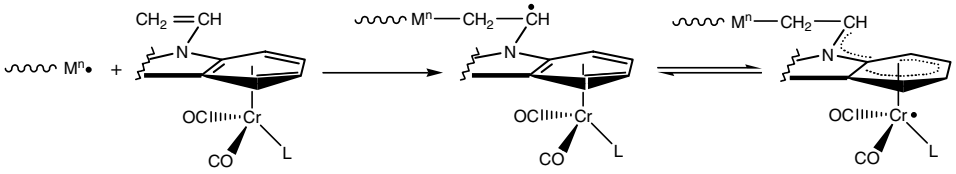

L = CO (**6**); PPh_3 (**7**)

Scheme 2.

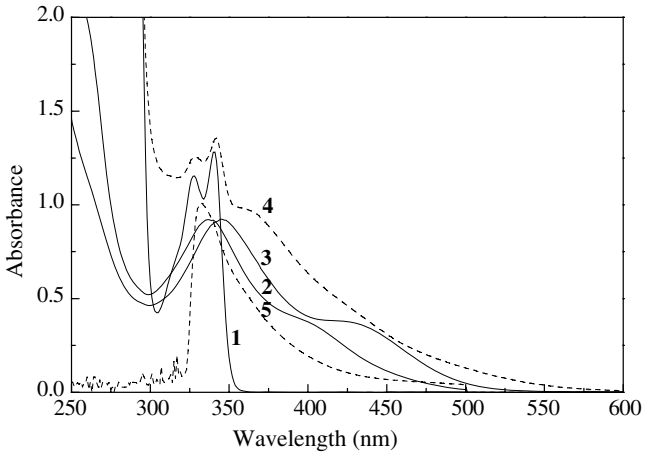

Fig. 9. Electronic absorption spectra of **1**–**4** in dichloromethane and **5** in acetone at 298 K.

transfer (MLCT) transitions (both $M \rightarrow \pi^*_{co}$ and $M \rightarrow \pi^*_L$) in accord with their negative solvatochromium and apparent sensitivity to the electronic nature of the ligands. As reported on the related system [5a,21], the MLCT transition band is expected to be smaller in its intensity owing to the non-coincidence of the ground-state dipole moment and the charge-transfer directions, it is reasonable to suggest that these transitions of the lower energy bands may contain considerable ligand field character on the basis of their fairly large molar absorptivities (Table 3). The higher energy bands immediately adjacent have higher extinction coefficients and can be regarded as the intraligand $\pi - \pi^*$ transition (IL). The change from **2** to **3** causes a subtle red-shift both in the lower energy band by 35 nm and the higher energy band by 8 nm. A plausible explanation is the electronic transitions within the dinuclear-carbazole ring system accompanied by the electronic communication between the two metal centers. Additional electron density from each chromium center may interact with the carbazole ligand in order to decrease the coordinative unsaturation, thereby increasing delocalization of the π electrons into the carbazole system. The differences in red-shift extent of MLCT and IL bands can be viewed as the population redistribution associated with the charge-transfer transition. These results would assist us in evaluating the question how well the electronic behavior of the coordinated carbazole ring was "matched" to that of the $Cr(CO)_3$ center. It seems likely that **3** would prove to be better matched because of a red-shift of its absorption bands relative to **2**, again consistent with the aforementioned conversion of **2** into **3** in solution. Replacing a CO with a phosphine ligand as in **4**, causes the low-energy band to have a large molar absorptivity and extend past 600 nm, but no observable changes occur in the high-energy band. This can be attributed to the addition effect of the extinction coefficients of the PPh_3 unit and the mixing of the intraligand (IL) $\pi - \pi^*$ (PPh_3) transition into the MLCT transition due to the lone-pair contribution from the phosphorus atom. Complex **5** exhibits a high-energy absorption band at about 330 nm with a long tail extending far into the visible. Perhaps the greater extent of the blue-shift for the MLCT band than the IL band, which was caused by the strong electron-withdrawing effect of $(C_3H_5)^+BF_4^-$ ligand, makes these two bands be substantially overlapping, and it is not accessible to accurately assign their positions. The electronic spectra of polymer **6** and **7** were also examined under the same conditions and show no clear difference in energy compared to their corresponding monomers (Fig. 10), suggesting that Cr-bound carbazole served as the pendant chromophore is practically unaffected by the vinyl-type polymerization due to their unconjugated polymer backbone.

All complexes in this work are emissive in a degassed solution at room temperature, and the emissive behaviors are sensitive to their concentration in the range from 10^{-3} to 10^{-5} mol dm^{-3}, but independent of the excitation

Table 3
Electronic absorption and emission data in dichloromethane at 298 K unless otherwise stated

Compound	λ_{max}, nm ($10^{-3}\varepsilon$, M^{-1} cm^{-1})	λ_{em}[b], nm ($10^2\Phi$)
1	328 (38), 341 (40)	353, 366sh (42)
2	337 (30), 395 (15)	353sh, 369 (3.8)
3	345 (30), 430 (16)	349, 364sh (1.7)
4	329 (41), 342 (42), 365 (32), 430sh (11)	353, 367sh (7.5)
5[a]	333 (33), 370sh (10)	394 (~0.09)
6	334 (30), 402 (15)	351, 366 (3.1)
7	332 (29), 343 (30)	354, 420sh (2.9)
PVK	330 (30), 344 (30), 363 (29), 398sh (22)	380, 420sh (56)

[a] Measured in acetone.
[b] The excitation wavelength is 315 nm.

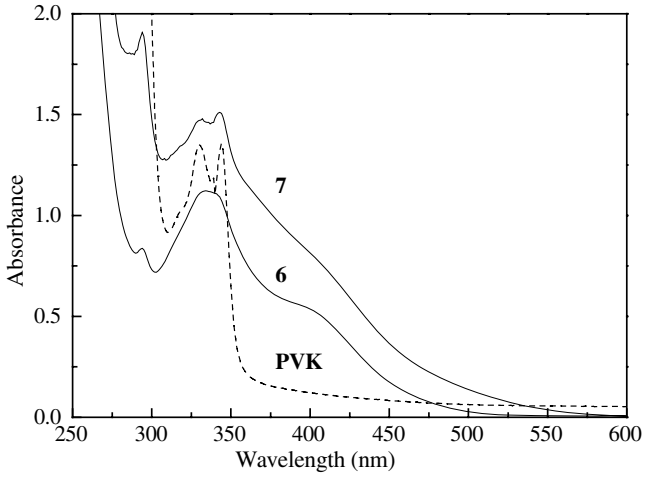

Fig. 10. Electronic absorption spectra of **6**, **7** and PVK in dichloromethane at 298 K.

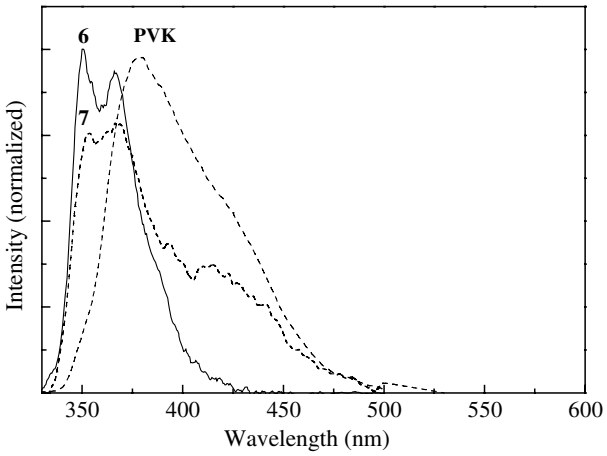

Fig. 12. Emission spectra of **6**, **7** and PVK in dichloromethane at 298 K.

wavelength used. The emissions of **2**–**4** appear in the same region and have structural features very similar to that of **1** (Fig. 11), suggesting the same source from the carbazole ligand-dominating emissive state. Thus their lowest emissive states can tentatively be assigned as metal-perturbed $\pi - \pi^*$ transitions. However, complex **5** shows broad emission with a maximum at 394 nm, whose behavior of the change in spectral shape and position is considered to originate from the significant perturbation of the cationic π-allyl ligand. In addition, we observed a notable but not dramatic quenching effect for these complexes as far as fluorescence quantum yields are concerned [22]. We can possibly attribute the quenching in the emission intensity to the so-called heavy-atom effect of the central chromium, which triggers the non-radiative deactivation of excited states of the fluorophore. Due to the lack of available low-lying metal-localized excited states [23], it is unlikely that energy or electron-transfer quenching mechanism operates here. The trend of the emission maxima decrease from **1** to **3** is consistent with the increased heavy-atom effect. It is also clear that variation of the ligands has somewhat of an influence on the emission intensity, wherein an order of $\mathbf{4} > \mathbf{2} > \mathbf{5}$ is expected on the basis of the different accepting capacities of the ligands, i.e., $PPh_3 < CO < (C_3H_5)^+BF_4^-$. Extension of the observations on these small-molecules to the macromolecular level is straightforward in Fig. 12. Polymer **6** totally manifests the emissive behavior of its parent complex **2**. No new emission bands appeared at a relatively longer wavelength excludes the possibility of an overlapping, eclipsed, sandwich-like conformation concerning excimer formation [24]. To our surprise, polymer **7** exhibits, in addition to the 350 nm monomer fluorescence, a structureless emission at $\lambda > 380$ nm which compares well with that observed for PVK. This is tempting to be excimer-like in its behavior whose origin undoubtedly results from the formation of an intrachain excimer state. Apparently, the very bulky $Cr(CO)_2PPh_3$ fragment does not sterically avert overlap of the pendant organometallic chromophores. These inspections led us to speculate that, irrespective of the steric compression, the electronic property of the ligand is also a crucial factor, which determines the appropriate disposition of two Cr-bound carbazole groups and the formation of excimers. Encouraged by these results, we are continuing our studies on these metallopolymers, in particular, their photophysical properties concerning themselves with the configurational requirements.

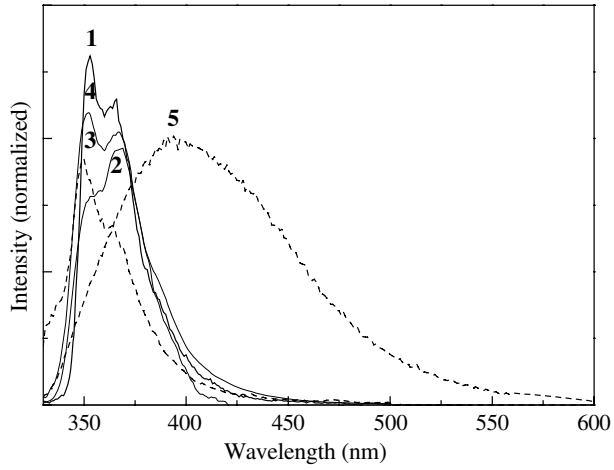

Fig. 11. Emission spectra of **1**–**4** in dichloromethane and **5** in acetone at 298 K.

4. Conclusion

We have shown the synthesis and isolation of mono- (**2**) and bis-$Cr(CO)_3$ (**3**) complexes of *N*-vinylcarbazole, which are well promising for optoelectronic applications because of their organometallic push–pull structures, ability of vinyl-type polymerization and versatility in structural modification following a rational exchange of a CO group. To our knowledge, it is also the first instance that conversion from **2** to **3** occurs upon heating

in coordinating solvents because **3** is thermodynamically more stable than **2**. The *N*-vinylcarbazole$Cr(CO)_2L$ complexes, where $L = PPh_3$ (**4**), $(C_3H_5)^+BF_4^-$ (**5**), are acquired as comparable products, which possess varying physico-chemical properties as these ligands exhibit different donor–acceptor properties ($(C_3H_5)^+BF_4^-$ is a very strong acceptor, CO is a strong π-acceptor and PPh_3 is a moderate donor and acceptor). Single-crystal X-ray structures were obtained for **2**–**4**. By structure–property correlation, the followings can be summarized as own conclusion. The *N*-vinyl double bond length seems rather sensitive to the electronic nature of the ligand, shortening by more than 0.029 Å upon the replacement of one CO group with PPh_3 ligand. The distances of Cr from the carbazole plane, which allows estimates of the strength of the metal–ligand π-bonding, are equal to each other for **2** and **4** but shorter for **3**. Electronic absorptions of these complexes extend over a wide range and can be varied by modifying the ligands. Furthermore, a subtle red-shift in absorption bands caused by change from **2** to **3** provides support for the electronic communication between the two $Cr(CO)_3$ groups on one carbazole unit. Despite a notable but not dramatic quenching effect, the emission properties of the complexes **2**–**4** hardly differ from each other and are similar to that of their organic counterpart **1**, suggesting the carbazole ligand-dominating emissive state. However, the emission profile of complex **5** changes dramatically due to a significant perturbation of the cationic π-allyl ligand. The polymerization behavior is proposed to be associated with the influence of the metal atom, which makes the organometallic radical or corre- sponding macroradical inert and of low polymerizability. Under radical initiation conditions, complexes **3** and **5** could not be polymerized, while complexes **2** and **4** displayed a controlled polymerization by the stable organometallic radical polymerization mechanism and gave the corresponding well-defined polymers **6** and **7**. An emission spectral examination of the resultant polymers provides notable insight into the fact that electronic effects of the ligands dominate the intrachain excimer formation, even those such as PPh_3 which are largely bulky. Further photophysical studies of these chromium–carbazole complexes and their polymers will be reported in due course.

Acknowledgments

We are grateful to the National Natural Science Foundation of China (Grant No. 20274011) for generous financial support. We thank Dr. Jie Sun for assistance in X-ray data collection and refinement of compounds **1**–**4**.

Appendix A. Supplementary data

Crystallographic data for the structural analysis has been deposited with the Cambridge Crystallographic Data Centre, CCDC No. 285129 for compound **2**, No. 285130 for compound **3**, No. 285131 for compound **4** and No. 285132 for compound **1**. Copies of this information may be obtained free of charge from The Director, CCDC, 12 Union Road, Cambridge, CB2 1EZ, UK (fax: +44 1223 336033; e-mail: deposit@ccdc.cam.ac.uk or http://www.ccdc.cam.ac.uk). Supplementary data associated with this article can be found, in the online version, at doi:10.1016/j.jorganchem.2005.10.052.

References

[1] J. Mort, G. Pfister, in: J. Mort, G. Pfister (Eds.), Electronic Properties of Polymers, Wiley Interscience, New York, 1982.
[2] V.S. Mylnikov, Adv. Polym. Sci. 115 (1994) 1.
[3] (a) G. Zotti, G. Schiavon, S. Zecchin, J.-F. Morin, M. Leclerc, Macromolecules 35 (2002) 2122;
(b) S.-W. Hwang, Y. Chen, Macromolecules 34 (2001) 2981;
(c) B. Andre, R. Lever, J.Y. Moisan, J. Chem. Phys. 137 (1989) 281;
(d) M. Yokayama, S. Shimokihara, A. Matsubara, H. Mikawa, J. Chem. Phys. 76 (1982) 724;
(e) C.I. Simionescu, V. Percec, G. Ioanid, Rev. Roum. Chim. 24 (1979) 1077.
[4] (a) J.P. Collman, L.S. Hegedus, J.R. Norton, R.G. Finke, Principles and Applications of Organotransition Metal Chemistry, University Science Books, Mill Valley, CA, 1987;
(b) W.E. Silxerthorn, in: F.G.A. Stone, R. West (Eds.), Advances in Organometallic Chemistry, vol. 13, Academic, New York, 1975, p. 48;
(c) J.E. Sheats, C.E. Carraher, C.U. Pittman Jr., Metal-containing Polymeric Systems, Plenum Press, New York, 1985;
(d) E.L. Muetterties, J.R. Bleeke, E.J. Wucherer, T.A. Albright, Chem. Rev. 82 (1982) 499;
(e) R.H. Crabtree, Chem. Rev. 85 (1985) 245.
[5] (a) K. Shen, X. Tian, J. Zhong, J. Lin, Y. Shen, P. Wu, Organometallics 24 (2005) 127;
(b) T.J.J. Müller, M. Ansorge, H.J. Lindner, Chem. Ber. 129 (1996) 1433.
[6] (a) C.A. Merlic, M.M. Miller, B.N. Hietbrink, K.N. Houk, J. Am. Chem. Soc. 123 (2001) 4904;
(b) C.A. Merlic, B.N. Hietbrink, K.N. Houk, J. Org. Chem. 66 (2001) 6738;
(c) C.A. Merlic, J.C. Walsh, D.J. Tantillo, K.N. Houk, J. Am. Chem. Soc. 121 (1999) 3596;
(d) S.G. Davies, T.J. Donohoe, Synlett (1993) 323;
(e) C. Michon, J.-P. Djukic, Z. Ratkovic, J.-P. Collin, M. Pfeffer, A. De Cian, J. Fischer, D. Heiser, K.H. Dötz, M. Nieger, Organometallics 21 (2002) 3519.
[7] (a) H. Kobayashi, M. Kobayashi, Y. Kaizu, Bull. Chem. Soc. Jpn. 46 (1973) 3109;
(b) H. Kobayashi, M. Kobayashi, Y. Kaizu, Bull. Chem. Soc. Jpn. 48 (1975) 1222;
(c) S.D. Worley, T.R. Webb, J. Organomet. Chem. 192 (1980) 139;
(d) P.G. Sennikov, V.A. Kuznetsov, A.N. Egorochkin, N.I. Sirotkin, R.G. Nazarova, G.A. Razuvaev, J. Organomet. Chem. 190 (1980) 167;
(e) R. Lal De, J. von Seyerl, L. Zsolnai, G. Huttner, J. Organomet. Chem. 175 (1979) 185.
[8] (a) M. Cais, M. Kaftory, D.H. Kohn, D. Tatarsky, J. Organomet. Chem. 184 (1979) 103;
(b) R. Dabard, G. Jaouen, G. Simonneaux, M. Cais, D.H. Kohn, A. Lapid, D. Tatarsky, J. Organomet. Chem. 184 (1980) 91;
(c) M.J. Wovkulich, J.D. Atwood, J. Organomet. Chem. 184 (1979) 77;
(d) G. Jaouen, R. Dabard, J. Organomet. Chem. 72 (1974) 377.
[9] (a) C.U. Pittman Jr., O.E. Ayers, S.P. McManus, Macromolecules 7 (1974) 737;
(b) C.U. Pittman Jr., R.L. Voges, J. Elder, Macromolecules 4 (1974) 302;

(c) C.U. Pittman Jr., G.V. Marlin, J. Polym. Sci. 11 (1973) 2753;
(d) C.U. Pittman Jr., P.L. Grube, O.E. Ayers, S.P. McManus, M.D. Rausch, G.A. Moser, J. Polym. Sci. A 10 (1972) 379.
[10] (a) G.M. Sheldrick, SHELXS-97, Program for Crystal structure Solution, Gottingen University, Germany, 1997;
(b) G.M. Sheldrick, SHELXS-97, Program for Crystal structure Refinement, Gottingen University, Germany, 1997.
[11] Y. Oprunenko, S. Malyugina, P. Nesterenko, D. Mityuk, O. Malyshev, J. Organomet. Chem. 597 (2000) 42.
[12] (a) T.A. Albright, P. Hofmann, R. Hoffmann, C.P. Lillya, P.A. Dobosh, J. Am. Chem. Soc. 105 (1983) 3396;
(b) E.P. Kündig, V. Grivet, C. Desobry, B. Spichiger, S. Rudolph, Organometallics 6 (1987) 1173;
(c) K.H. Dötz, J. Stendel Jr., S. Müller, M. Nieger, S. Ketrat, M. Dolg, Organometallics 24 (2005) 3219.
[13] (a) S.C. Jones, T. Hascall, S. Barlow, D. O'Hare, J. Am. Chem. Soc. 124 (1998) 11610;
(b) S. Barlow, D. O'Hare, Chem. Rev. 97 (1997) 637.
[14] R.D. Rogers, J.L. Atwood, T.A. Albright, W.A. Lee, M.D. Rausch, Organometallics 3 (1984) 263.
[15] (a) A.D. Hunter, L. Shilliday, W.S. Furey, M.J. Zaworotko, Organometallics 11 (1992) 1550;
(b) A.D. Hunter, V. Mozol, S.D. Tsai, Organometallics 11 (1992) 2251;
(c) J. Li, A.D. Hunter, R. McDonald, B.D. Santarsiero, S.G. Bott, J.L. Atwood, Organometallics 11 (1992) 3050.
[16] (a) M. Ansorge, T.J.J. Müller, J. Organomet. Chem. 585 (1999) 174;
(b) Y. Huang, H.L. Uhm, D.F.R. Gilson, I.S. Butler, Inorg. Chem. 36 (1997) 435;
(c) T.E. Bitterwolf, Polyhedron 7 (1988) 1377.
[17] (a) D.F. Grishin, L.L. Semyonycheva, A.N. Artemov, E.V. Telegina, N.B. Valetova, I.S. Illichev, Appl. Organometal. Chem. 17 (2003) 717;
(b) D.F. Grishin, L.L. Semyonycheva, I.S. Illichev, A.N. Artemov, Appl. Organometal. Chem. 15 (2001) 169.
[18] (a) A.D. Pomogailo, V.S. Savostyanov, Synthesis and Polymerization of Metal-containing Monomers, CRC Press, Boca Raton, 1994;
(b) D.F. Grishin, Russ. Chem. Rev. 62 (1993) 951.
[19] (a) C.A. Merlic, M.M. Miller, Organometallics 20 (2001) 373;
(b) D.J. Tantillo, B.N. Hietbrink, C.A. Merlic, K.N. Houk, J. Am. Chem. Soc. 122 (2000) 7136;
(c) T.G. Traylor, M.J. Goldberg, J. Am. Chem. Soc. 109 (1987) 3968.
[20] The EI-MS spectrum of the parent complex **4** shows the ($CrPPh^{3+}$) ion as the thermodynamically more stable fragment with the highest intensity, implying the strength of the phosphorus-binding pattern.
[21] (a) D.R. Kanis, M.A. Ratner, T.J. Marks, J. Am. Chem. Soc. 114 (1992) 10338;
(b) T.M. Gilbert, F.J. Hadley, C.B. Bauer, R.D. Rogers, Organometallics 13 (1994) 2024;
(c) T.J.J. Müller, J. Blümel, J. Organomet. Chem. 683 (2003) 354.
[22] Y. Morisaki, H. Chen, Y. Chujo, J. Organomet. Chem. 689 (2004) 1271.
[23] Excitation into the MLCT absorption ($\lambda > 450$ nm) band does not result in any emission.
[24] (a) A. Karali, P. Dais, E. Mikros, F. Heatley, Macromolecules 34 (2001) 5547;
(b) H. Sahai, A. Itaya, H. Masuhara, K. Sasaki, S. Kawata, Polymer 37 (1996) 31;
(c) G.E. Johnson, J. Chem. Phys. 62 (1982) 4697.